Navarro-Peris, E.; Álvarez-Piñeiro, L.; Schnabel, L.; Corberán, JM. (2021). Refrigerant maldistribution in brazed plate heat exchanger evaporators. Part B: Analysis of the influence of maldistribution on the evaporator performance. International Journal of Refrigeration. 131:312-321. https://doi.org/10.1016/j.ijrefrig.2021.04.003

Refrigerant maldistribution in brazed plate heat exchanger evaporators. Part B: Analysis of the influence of maldistribution on the evaporator performance

Emilio Navarro-Peris [1*], Lucas Alvarez-Piñeiro[1], Lena Schnabel[2], Jose M Corberan[1].

[1]Energy Engineering Institute, Universitat Politecnica de Valencia, Valencia, Spain.

[2]Fraunhofer Institute for Solar Energy Systems, Freiburg, Germany.

*Corresponding author: e-mail: emilio.navarro@iie.upv.es

Tel: (+34) 963879123

Abstract

The maldistribution of the refrigerant mass flowrate among the different channels of a brazed plate heat exchanger evaporator with distributor, has been studied with a thermographic camera working under different conditions of inlet vapor quality, superheat, and water temperature drop. Part A of this work includes the description of the experimental campaign and a full discussion of the obtained results. This paper (part B) presents, first an evaluation of the penalty caused by the refrigerant maldistribution on the evaporator performance, and the effect of the operation conditions on that penalty; second, a data reduction methodology, which allows the quantification of the maldistribution based on a series of simple assumptions and the flow conservation equations. Finally, given that it has been found that the water temperature drop across the evaporator has a strong influence on the performance penalty due to refrigerant maldistribution, the water temperature evolution is analyzed in detailed and the reasons for its great influence are explained and commented. On this regard, it is concluded that the penalty of the maldistribution on the evaporation performance strongly depends on the availability of the secondary fluid in the channels where most of the refrigerant liquid is concentrated. The described data reduction methodology, based on the analysis of the thermographies and the measured evaporator performance, is suitable to give an estimate of the maldistribution which seems reasonable and consistent with the observed data.

Keywords: Brazed plate heat exchanger, evaporator, refrigerant maldistribution, efficiency

Nomenclature

B	Constant in the Chisholm expression for the pressure drop across thin plates. Value 0.61
COP	Coefficient of performance (-)
COP_C	Theoretical Carnot cycle coefficient of performance (-)
C_p	Specific heat [J/(kg K)]
dTw	Water temperature drop (K)
L	Position along the evaporator [0-L] (m)
$\dot{m}_w$	Water mass Flow (kg s^{-1})
$\dot{m}_{ref}$	Refrigerant mass flowrate (kg s^{-1})
SH	Superheat (K)
T	Temperature (ºC)
T_{evap}	Evaporation temperature (ºC)
T_{cond}	Condensation temperature (ºC)
T_{min}	Minimum temperature registered in the thermography (ºC)
x	Vapor quality (-)

Greek symbols

η_C	Carnot efficiency (-)
α	Channel ratio between the number of channels of part I of the evaporator and the total number of channels (-)
β	Refrigerant mass flow ratio between the mass flowrate passing through part I of the evaporator and total refrigerant mass flowrate (-)
$\psi = \frac{1-\beta}{1-\alpha}$	Maldistribution index = ratio in between the actual refrigerant mass flowrate through part II of the evaporator and the one that would correspond to an even distribution of the refrigerant

Subscripts

in	inlet
o	outlet
w	water
v	vapor
l	liquid
ref	refrigerant
$evap$	evaporator
$cond$	condenser
I	Part I of the evaporator
II	Part II of the evaporator

1. Introduction

The use of brazed plate heat exchangers (BPHEs) as evaporators has hugely increased in the past years because of their high compactness and effectiveness. The most important problem degrading BPHE performance as evaporators is the maldistribution of the refrigerant mass flowrate among the channels. In the Part A of this work, an extensive experimental campaign about the dependence of refrigerant maldistribution on the operating conditions, based on thermographies, and performance testing, has been presented and the corresponding results analyzed in detail.

Most of the studies in the Literature about the problem of the maldistribution of the refrigerant mass flowrate among the different refrigerant channels have been carried out in micro channel evaporators (Brix et al., 2010, 2009; Gong et al., 2008; Kærn et al., 2011; Stevanovic et al., 2012), or in fin and tube evaporators (Bach et al., 2013; Choi et al., 2003; Mader et al., 2015) showing that the maldistribution in the air side has even a higher impact on the system performance than the maldistribution in the refrigerant side and reporting estimations of the COP degradation ranging from 5% to 40% depending on the evaporator and conditions analyzed.

Regarding maldistribution in BPHEs, the studies are more scarce, but some recent studies brought new information. (Li and Hrnjak, 2018) developed a validated model for single-phase flow distribution in PHEs, showing that plates with higher length-to-width ratios are less affected by maldistribution. Two-phase flow maldistribution in BPHEs was addressed by a few studies. (Jin and Hrnjak, 2017) investigated the in-channel distribution of R245fa experimentally but the detailed influence on the system performance was not addressed in this work. (Mancini et al., 2019) presented a model of BPHE working as evaporator, which is able to simulate the mass flowrate in each channel and estimate the influence on the evaporator performance, but the presented results are limited to specific working conditions and based on a hypothetical linear distribution of the vapor inlet quality which is not justified experimentally.

In summary, the maldistribution of refrigerant has been studied in a number of previous research works, however, the experimental ones are usually limited to remark the existence of the maldistribution, and to serve as contrast to validate some model aimed to assist the redesign the evaporator to improve the distribution. The developed mathematical models are based on the assumption of one-dimensional flow along the individual refrigerant channels, and on finding the refrigerant flow rate per channel balancing the total pressure drop. However, they also need the assumption of some additional hypothesis, usually about the vapor inlet quality, which clearly conditions the solution.

After the presentation and comment of the results of the extensive experimental characterization campaign carried out in part A, this paper presents for the first time, an in-depth analysis of the influence of the refrigerant maldistribution on the evaporator performance, i.e. on the evaporation temperature, and an analysis of the influence of the operating conditions on the refrigerant maldistribution, all over a wide range of conditions. In addition, a new data reduction methodology, based on a simplified model, and able to quantify the maldistribution from test data and the thermography, is presented, and has been used to characterize the evaporator performance as a function of the operating conditions.

2. Degradation of performance due to refrigerant maldistribution

As it has been described in Part A, the results of the experimental campaign show that the thermal distribution is clearly not even, among the channels, and that the evaporation temperature is affected by that maldistribution because a big portion of the liquid refrigerant seems to concentrate in a reduced number of channels (approximately 33% in the studied evaporator). However, it is clear that the evaporation temperature also depends on the operating conditions, mainly on the parameters taken as independent in the study, which are the evaporator inlet quality, the superheat, and the water temperature drop across the evaporator. In order to be able to isolate the different effects affecting the evaporation temperature and evaluating which part of the observed degradation is due to the refrigerant maldistribution among the channels, it is necessary

to compare the measured values with the values which could be attained with an even distribution of the refrigerant. As this is not possible with a real BPHE evaporator, a detailed mathematical model for BPHEs was used to generate those results. The employed BPHE model forms part of the IMST-ART software (Corberan et al., 2002). A full description of its characteristics and capabilities can be found in [www.imst-art.com].

The numerical method employed in the BPHE model is called SEWTLE (for Semi Explicit method for Wall Temperature Linked Equations). For a complete description of the numerical methodology see (Corberán et al., 2001). Dedicated empirically adjusted correlations are employed for the evaporation and condensation, local heat transfer and pressure drop, coefficients in BPHEs (García-Cascales et al., 2007)

The model has been validated in several studies and it is typically able to predict evaporation temperature with a high accuracy +- 1K. The inputs to the model are, first all the geometrical dimensions of the plates, the number of plates, the corrugation angle, the pitch, the plate thickness and the ports dimensions, as well as the diameter of the distributor orifices; Then, the operating conditions, which in this case were selected as: the measured refrigerant mass flow rate, the superheat, the water inlet temperature, and the water temperature drop across the evaporator. The model is able to estimate all the other corresponding outputs: the evaporation temperature, the heat transferred, the water mass flow rate, and the detail of temperature, vapor quality and pressure evolution all along the refrigerant and water channels, as well as the local heat transfer coefficients and friction factors. The model assumes uniform refrigerant distribution in the evaporator, so that the estimation of the evaporation temperature will serve as reference for the operation of the evaporator free of refrigerant maldistribution.

Figures 1 and 2 show the comparison of the measured evaporation temperature with the value estimated with the model with uniform distribution, for each test point, with the superheat in the X-axis, for the cases of dTw=5 K and dTw=13 K, respectively. The values estimated with the model are represented with empty symbols whereas the measured ones employ solid ones. In order to improve the visibility, the experimental values have been drawn with joining lines. A

grey color dotted line has been also included. This line represents the upper limit for the evaporation temperature (T_{evap} max) just taking into account that in countercurrent flow the evaporation temperature must be lower than either the outlet water temperature ($Tw_o=Tw_{in}-dTw$) or the inlet water temperature minus the superheat ($Twin-SH$).

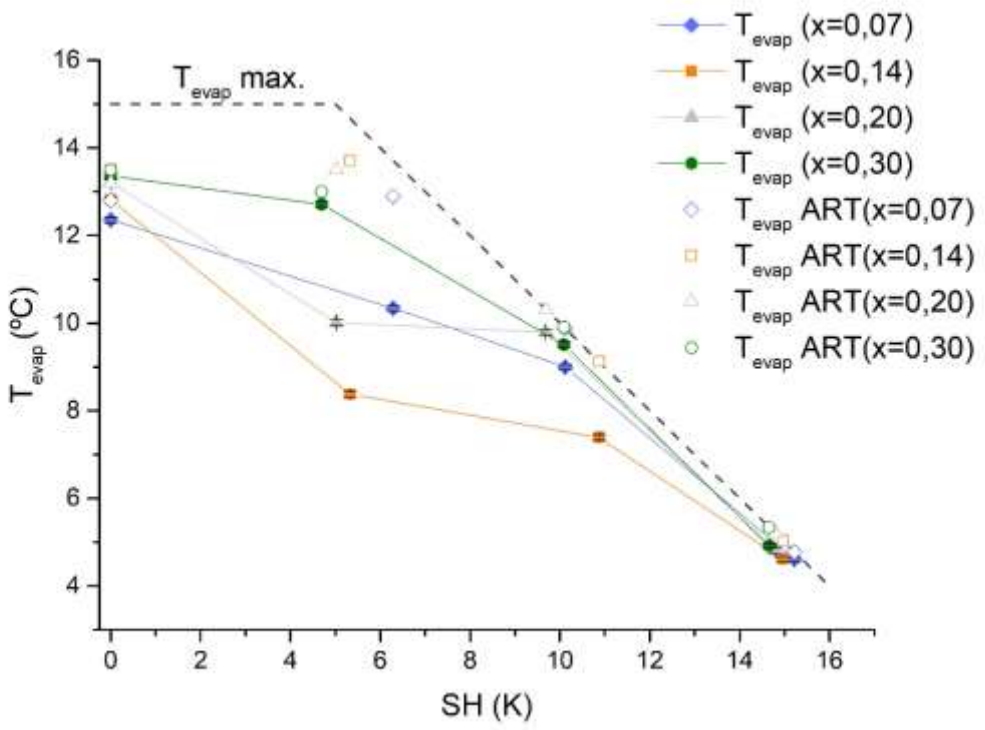

Figure 1. Measured vs. calculated evaporation temperature for the tests with water temperature drop (dTw) around 5K

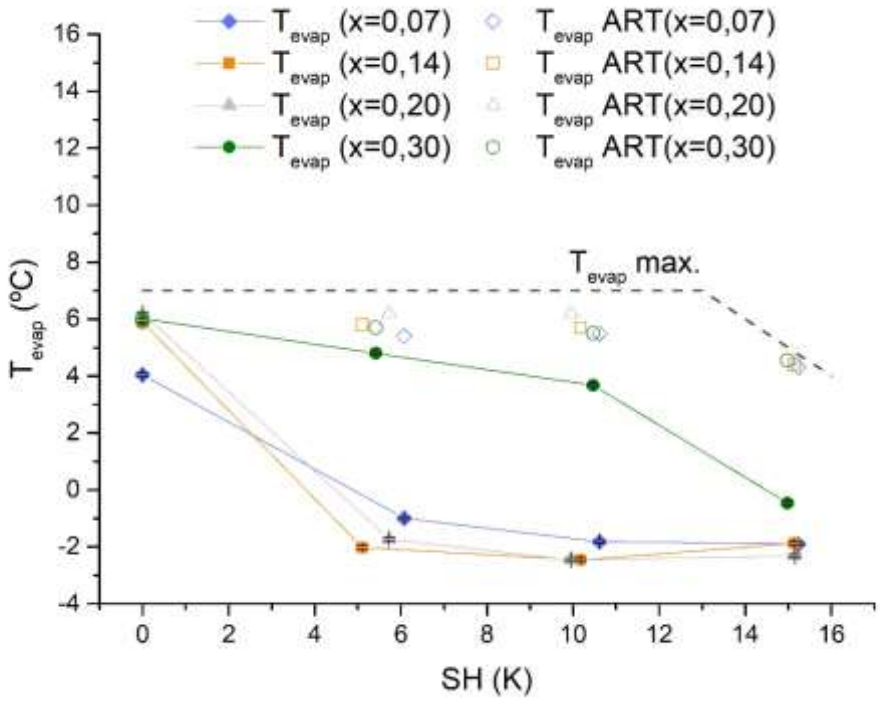

Figure 2. Measured vs. calculated evaporation temperature for the tests with water temperature drop (*dTw*) around 13K

As can be observed, the experimental values are in general much lower than the calculated ones. The agreement between calculated and measured values is only good at null superheat. At those conditions, however, it seems there is still a deviation, with lower evaporation temperatures in the test points with the lowest inlet qualities, with a high deviation for *dTw*=13 K and inlet quality *x*=0.07.

On the other hand, independently of the water temperature drop, both calculated and measured values are almost coincident when the evaporation temperature is controlled by the superheat, with an evaporation temperature very close to Twin-SH. When the superheat is very high, the evaporation temperature is controlled by the large value of the superheat, and the fact that most of the evaporator area is dedicated to superheating, makes that the refrigerant maldistribution, although present does not produce a further penalty on the evaporation temperature. This is also possible to be distinguished in the thermographies, where, at the highest superheats, the outlet of

part II (see the division of the evaporator in part I and II in Figure 4), which we assumed with a high content of liquid refrigerant, is seen as superheated.

It is also interesting to note that for *dTw*=5 K, the cases with high quality inlet, 0.2 and 0.3, also present a good agreement with the calculated results, clearly indicating a lower penalty due to the maldistribution. However, at *dTw*=13 K this is only appreciable at inlet quality 0.3, which clearly presents a penalty lower than for the other inlet qualities. Therefore, the penalty due to the maldistribution depends on the inlet quality.

Figure 3 represents the difference between the calculated evaporating temperature with the detailed model and the measured evaporating temperature, as a function of the inlet vapor quality and superheat. This difference could be therefore seen as the penalty on the evaporation temperature due to the refrigerant maldistribution.

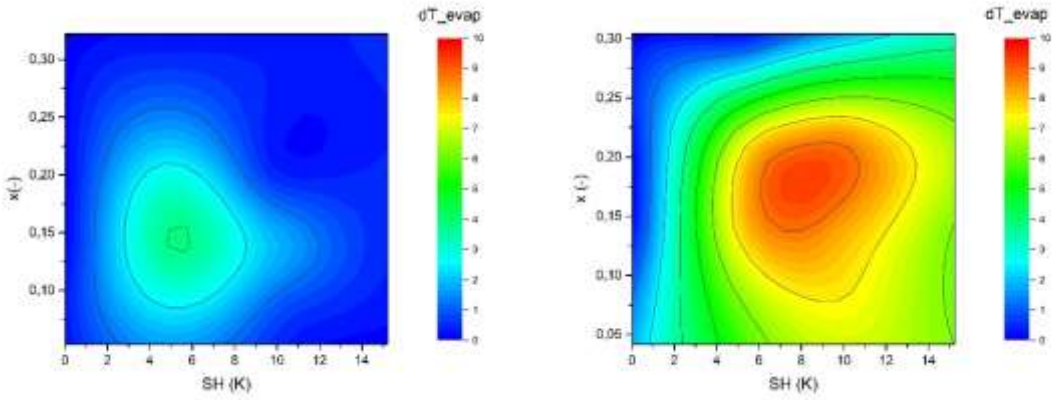

Figure 3. Difference between the calculated evaporating temperature and the measured evaporating temperature, for dTw = 5 K (left). and dTw= 13 K (right), for different superheats and inlet vapor qualities.

In all the cases, the estimated temperature by the model is similar or higher than the measured evaporating temperature. Figure 3 (left) shows that for water temperature drops of 5 K the evaporating temperature is only significantly lower than the estimated one for the case in which the superheat is around 5 K (3 to 7 K) and the vapor quality has values between 0.1 and 0.2. Therefore, in this case, although the thermography pictures show an uneven distribution of the refrigerant, it only has a significant impact in the evaporator performance for superheat values around 5 K. In contrast, Figure 3 (right) shows that for water temperature drops of 13 K the

evaporator performance is significantly different from the expected behavior with even distribution, and it shows a significant degradation of the evaporation temperature for all conditions except for the left upper corner with the highest inlet quality and the lowest superheat. The highest degradation occurs at superheats around 8 K (6 to 10) and vapor qualities between 0.12 and 0.22. Finally, it should be pointed out that, in practice, no degradation due to refrigerant maldistribution is observed for the case of superheat 0 K consistently with the quite even temperature distribution seen in the thermographies.

The penalty on the system performance due to a drop in the evaporation temperature can be estimated through a simple procedure, considering the effect of the evaporation temperature drop in the variation of the *COP* of the Carnot theoretical cycle $COP_C = \frac{T_c}{T_c - T_e}$, in the following way:

$$\frac{\partial COP}{\partial T_e} = \frac{d}{dT_e}(\eta_C \cdot COP_C) = \eta_C \cdot COP_C \cdot \frac{1}{T_c - T_e} = COP \cdot \frac{1}{T_c - T_e}$$

$$\frac{\Delta COP}{COP} \cdot 100 = \frac{\Delta T_e}{T_C - T_e} \cdot 100 \qquad (1)$$

Which is based on the assumption that the Carnot efficiency of the cycle, defined as $\eta_C = \frac{COP}{COP_C}$, remains approximately the same for small changes of the evaporation or condensation temperatures. Applying equation 1, the penalty on COP due to maldistribution can be estimated, leading to exactly the same representation of Figure 3 since the penalty on COP is mainly proportional to the evaporation temperature difference ΔT_e. Maximum COP degradation is 10% at superheat 5 K and inlet quality 0.14 for the case of *dTw* = 5 K, while it is 17% for the case of *dTw* = 13 K at superheat 10 K and inlet quality 0.20, values which clearly represent a very high degradation of the unit efficiency.

3. Temperature evolution and maldistribution analysis

The answer to the questions arisen above is obviously that the maldistribution is strongly affecting the heat exchange at the evaporator, by concentrating a large fraction of the liquid refrigerant in a small portion of the channels, as it is concluded from the observation of the thermographies.

However, it is difficult to explain the reason why the effect on the penalty of the evaporation temperature, and consequently on the unit *COP*, is so affected by the water temperature drop across the evaporator. In order to analyze and try to quantify this influence a study of the water temperature evolution was performed.

The observation and analysis of the thermographies indicated that it seems that there is a region, in most of the cases at the end of the distributor, which concentrates if not all, a large fraction of the liquid refrigerant, and that this region approximately corresponds to 1/3 of the channels. Further analysis of the thermographies allowed us to find out that the lowest temperature of the thermography is always found at the bottom of that region, exactly close to the outlet of the water channels flowing into the bottom header. Furthermore, the thermography always captures with high accuracy the lowest value of the temperature map, and that minimum temperature always corresponds with the temperature at the mentioned point. Table 1 shows the value of the registered minimum temperature of the thermography for each test point. If one compares these values with the values of the evaporation temperature for each case (shown below the minimum temperature in the table), it is easy to see that the evaporation temperature is always lower. For the cases with dTw=5 K and low superheat the evaporation temperature is only slightly lower, with the difference increasing with superheat. For the cases with dTw=13 K, the differences with the evaporation temperatures are already large at superheat null but they are almost constant (about 1K) at higher superheats.

Table 1. Minimum temperature (Tmin) of the each thermography and the corresponding evaporation temperature

T_{min}(ºC)	dT_w=5 K				dT_w=13K			
T_{evap}(ºC)	SH (K)				SH (K)			
x (-)	0	5	10	15	0	5	10	15
0.04	**14.5** 12.34	**13.2** 10.34	**12** 9.0	**11** 4.61	**11** 4.04	**-0.1** -1.02	**-1** -1.8	**-1** -1.88
0.14	**16.6** 12.81	**11.1** 8.37	**10.4** 7.39	**10.4** 4.61	**8** 5.97	**-1.1** -2.02	**-1.1** -2.46	**-0.5** -1.88
0.2	**16** 13.38	**12.4** 10.01	**12.7** 8.17	**9.2** 4.8	**9** 6.2	**2.5** 1.5	**-1.3** -2.45	**-1.5** -2.31
0.3	**15** 13.34	**14.1** 12.71	**13.4** 9.5	**10.7** 4.92	**9** 6.04	**5.4** 4.8	**4.4** 3.67	**0.5** -0.46

If one assumes now that the minimum temperature registered at the thermographies could be indicative of the water temperature, that minimum value would correspond, as it is also clear in the thermographies, to the water outlet temperature (T_{wo_II}) of the channels that concentrate most of the liquid refrigerant (part II of the evaporator). The low value of the water at the outlet being then explained by the fact that the water circulating through the water channels of that part of the evaporator are providing the heat for the evaporation of most of the liquid refrigerant.

Based on the observation of the thermographies and the measured variables, the following data reduction methodology for the maldistribution quantification has been developed. When maldistribution is present, the evaporator can be divided in two heat exchangers working in paralel at the same evaporating temperature (see Figure 4 as an example); part II where the refrigerant reaches the evaporator outlet in two-phase, and part I where the refrigerant is clearly superheated in a large fraction of the channel.

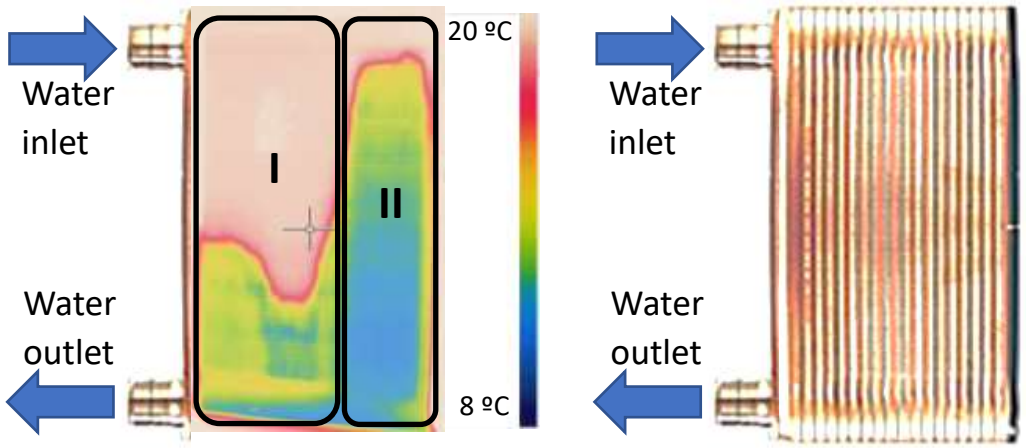

Figure 4. Division of the evaporator in two parts, I and II, based on the thermography results (left). Image of a brazed plate heat exchanger from the side in which the thermography is taken (right).

Based on the whole set of thermographies with clear maldistribution, one can assume that part I approximately occupies 2/3 of the channels and part II the other 1/3 (see part A, Navarro-Peris et al.). If additionally, one a ssumes that the water is quite evenly distributed among the channels it is possible to evaluate the water mass flowrate flowing through the channels of part I and part II:

$$\dot{m}_{w-I} = \alpha \cdot \dot{m}_w = \frac{2}{3} \cdot \dot{m}_w$$

$$\dot{m}_{w-II} = (1-\alpha) \cdot \dot{m}_w = \frac{1}{3} \cdot \dot{m}_w$$

Where α is the fraction of channels of part I, and correspondingly (1- α) is the fraction of channels of part II (2/3 and 1/3, in this case as commented above).

The conservation of vapor and liquid at the inlet of the evaporator requires

$$x_{in} = \beta \cdot x_{in-I} + (1-\beta) \cdot x_{in-II}$$

where x_{in} represents the vapor quality at the inlet of the evaporator, x_{in-I} the quality at the inlet to part I, x_{in-II} the quality at the inlet to part II, and β the refrigerant mass flow ratio between the

refrigerant mass flowrate passing through part I of the evaporator and the total refrigerant mass flowrate.

$$\beta = \frac{\dot{m}_{ref\_I}}{\dot{m}_{ref}}$$

Assuming now that the heat exchanged with the water at part II of the evaporator is employed to evaporate all the liquid refrigerant entering that part, and that the refrigerant is almost in saturated conditions at the outlet of that part, the following heat balance equation can be stated:

$$(1-\alpha)\cdot \dot{m}_w \cdot C_p \cdot \left(T_{win} - T_{wo\_II}\right) = (1-\beta)\cdot \dot{m}_{ref} \cdot (1 - x_{in-II}) \cdot (h_v - h_l)$$

Finally, neglecting the pressure drop along the refrigerant channels, and employing the Chisholm's expression for pressure drop of thin plates (Chisholm, 1983) for the evaluation of the pressure drop across the distributor orifice situated at the entrance of each refrigerant channel, the system of equations can be closed by stating that the pressure drop through the orifice must be equal for parts I and II:

$$\left(\frac{\beta}{\alpha}\right)^2 \left[1 + \left(\frac{\rho_l}{\rho_v} - 1\right)\left(B \cdot x_{in-I} \cdot (1 - x_{in-I}) + {x_{in-I}}^2\right)\right]$$

$$= \left(\frac{1-\beta}{1-\alpha}\right)^2 \left[1 + \left(\frac{\rho_l}{\rho_v} - 1\right)\left(B \cdot x_{in-II} \cdot (1 - x_{in-II}) + {x_{in-II}}^2\right)\right]$$

Where B is a constant that for thin plates has the value of 0.61 (Chisholm, 1983).

With this three equations and having as inputs the values from the experiments of the water outlet temperature at part II (T_{wo_II}) shown in Table 1, the evaporation temperature, and the value of α from the thermographies, the values of $x_{in\text{-}I}$, $x_{in\text{-}II}$ and β can be obtained for each experiment. The values of $x_{in\text{-}I}$, $x_{in\text{-}II}$ give an idea about the assimetry in the vapor quality distribution between the two parts of the evaporator, while the value of $\frac{1-\beta}{1-\alpha}$ is a quantification of the maldistribution, that we will call 'maldistribution index, ψ', since it is the ratio in between the actual refrigerant mass

flowrate flowing through part II of the evaporator and the one that would correspond to an even distribution of the refrigerant:

$$\psi = \frac{\frac{\dot{m}_{ref\_II}}{(1-\alpha)}}{\frac{\dot{m}_{ref}}{1}} = \frac{\frac{\dot{m}_{ref\_II}}{\dot{m}_{ref}}}{1-\alpha} = \frac{1-\beta}{1-\alpha}$$

A value of the maldistribution index ψ of 1 means even distribution.

Table 2 gives the results of those calculations for all test points of *dTw*=5 K and superheat around 5 K and for all the tests points of *dTw*=13 K, in which it is seen in the thermographies that the low temperature region in part II reaches the top of the evaporator, and therefore the adopted assumptions are reasonable.

Table 2. Maldistribution characteristic parameters obtained for each test point.

dTw (K)	SH (K)	β (-)	x_{in-I} (-)	x_{in} (-)	x_{in-II} (-)	ψ (-)
4.6	6.3	0.51	0.140	0.078	0.013	1.43
5.4	5.3	0.49	0.253	0.141	0.036	1.52
4.3	5.0	0.47	0.348	0.191	0.052	1.56
4.6	4.7	0.60	0.382	0.322	0.232	1.17
13.2	6.1	0.50	0.120	0.064	0.009	1.48
13.1	5.1	0.50	0.235	0.139	0.045	1.49
12.7	5.7	0.60	0.311	0.209	0.095	1.17
13.1	5.4	0.63	0.317	0.291	0.246	1.09
12.9	10.6	0.45	0.146	0.069	0.004	1.60
13.0	10.2	0.48	0.248	0.139	0.039	1.54
12.5	10.0	0.48	0.367	0.215	0.075	1.53
13.2	10.5	0.61	0.351	0.304	0.231	1.15
12.9	15.2	0.44	0.157	0.072	0.004	1.63
13.0	15.1	0.48	0.250	0.141	0.041	1.53
12.8	15.2	0.47	0.353	0.199	0.063	1.56
13.1	15.0	0.53	0.387	0.268	0.133	1.38

As can be seen in Table 2, the results indicate that the vapor quality at the entrance of part II is as it had been speculated, quite low, indicating that this part is flooded with liquid refrigerant, except for the highest inlet qualities where it seems there exists a better distribution. The maldistribution index ψ is always considerably greater than 1, reaching a maximum of 1.63.

Figure 5 shows the vapor quality at the entrance of part II vs. the inlet vapor quality to the evaporator, for the different series of test points considered, while Figure 6, shows the maldistribution index results. As can be seen in Figure 5, the values of the vapor quality at the inlet of part II are below 0.05 for most of the cases, in agreement with the observation of the liquid refrigerant accumulating in that part of the evaporator. However, when the vapor quality at the inlet of the evaporator (X-axis) goes beyond 0.2 there is a clear increase, with the vapor quality entering part II, approaching then the diagonal in the graph, what indicates an even distribution of the vapor quality. All series show more or less the same trend, so indicating a certain independence on the other operating conditions: superheat SH, and water temperature drop dTw. Figure 6 shows that the maldistribution index ψ is around 1.5 at vapor inlet qualities lower than 0.3, meaning that the refrigerant mass flowrate through part II of the evaporator is 50% higher than the one it would circulate if there were even distribution of the refrigerant among the channels. The maldistribution shows a clear trend to decrease for inlet vapor qualities above 0.2, approaching even distribution for qualities above 0.3.

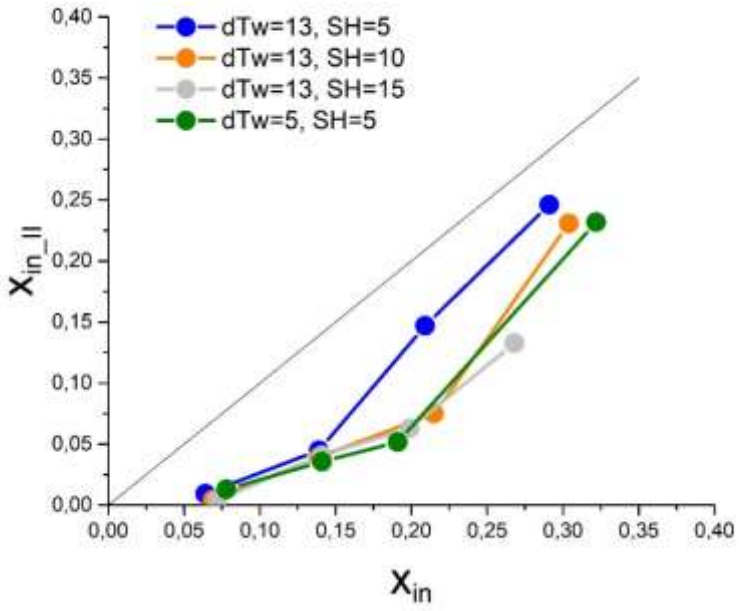

Figure 5. Vapor quality at the entrance of part II vs. the evaporator inlet vapor quality.

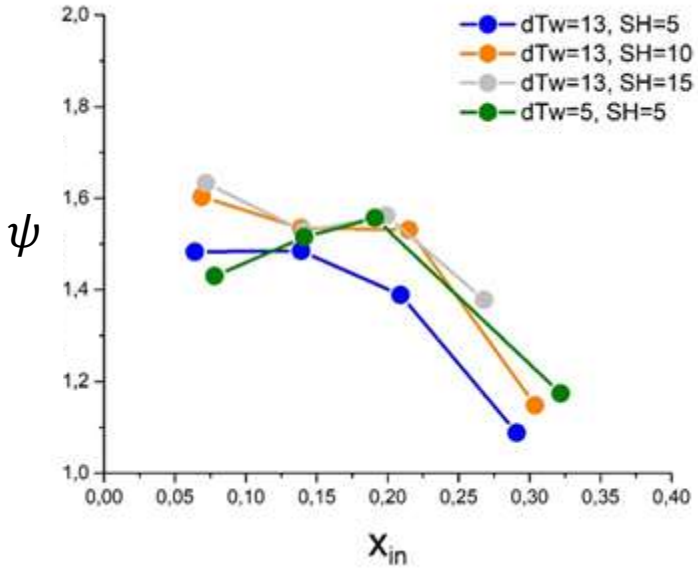

Figure 6. Values of the maldistribution index ψ vs the vapor inlet quality

The fact that the distribution of refrigerant at high qualities is quite even is probably due, first the fact that at high qualities there is a better distribution of the droplets in the distributor , as it has been reported by other authors, e.g. (Vist and Pettersen, 2004), and second, to the corrector effect of the distributor orifices that usually incorporate the evaporators at the inlet of the refrigerant channels exactly with that purpose, and which is optimized for the typical inlet qualities in evaporators (20 - 30%). However, it is important to point out that, as seen in the present study, the orifices are not able to even the distribution in applications with low inlet qualities, at it is the case of units with high subcooling.

The fact that the maldistribution estimated values are similar and quite independent of the water temperature drop is an important result. Indeed, it was logical to expect that changes on the water side should not affect the maldistribution of refrigerant. Still, it was clearly found that *dTw* has a strong effect on the penalty of the maldistribution on the evaporator performance. In order to investigate this, a comparison between the measured temperatures and the ones calculated with the detailed model (IMST-ART) was performed again for some of the test points. For this, the estimated values of the inlet conditions to the refrigerant and water channels of both, part I and part II, obtained from the above described data reduction methodology, were employed as inputs

to the detailed evaporator model to estimate the evolution of the fluids across Part I and Part II heat exchangers, considered as two independent evaporators working at the same evaporation temperature. Figures 7, 8 and 9 show the calculated temperature evolution of the refrigerant, water, and of the plate in between both, compared with the temperature registered at the corresponding thermography along a vertical line drawn at the middle of part I and Part II, respectively. Figure 7 shows the results for the test point with x_{in}=0.2 and null superheat, *SH*=0 K, for the two analyzed cases of water temperature drop across the evaporator, *dTw*=5 K (left) and *dTw*=13 K (right). It should be reminded that for null superheat the thermograhies show a good refrigerant distribution with similar behavior among all the channels regardless the water temperature drop. Figure 8 shows the results for the test point with x_{in}=0.14, *SH*=5 K and *dTw*=5 K for both parts of the evaporator I (left) and II (right), while Figure 9 shows the results corresponding to the test point with x_{in}=0.20, *SH*=15 K and *dTw*=13 K, again for both parts I and II.

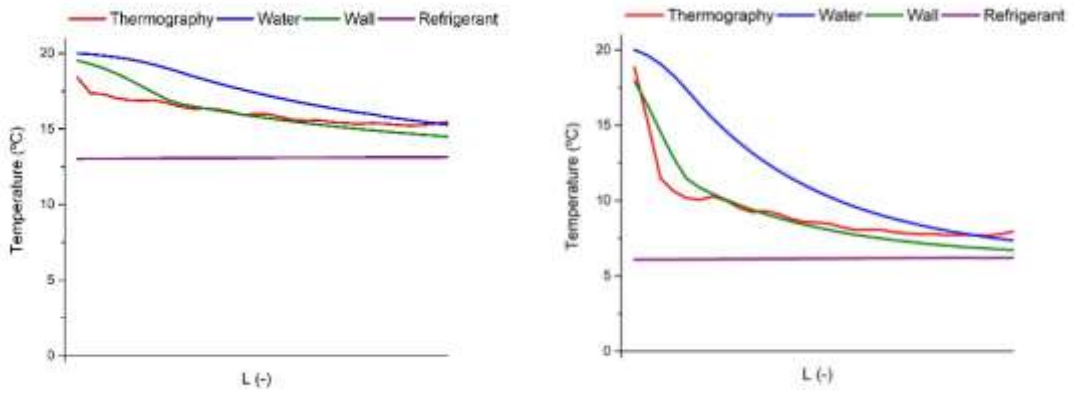

Figure 7. Comparison between the calculated temperature evolution and the one corresponding to the thermography for the test point with x_{in}=0.2, SH=0 K and dTw=5 K, (left), and dTw=13K(right).

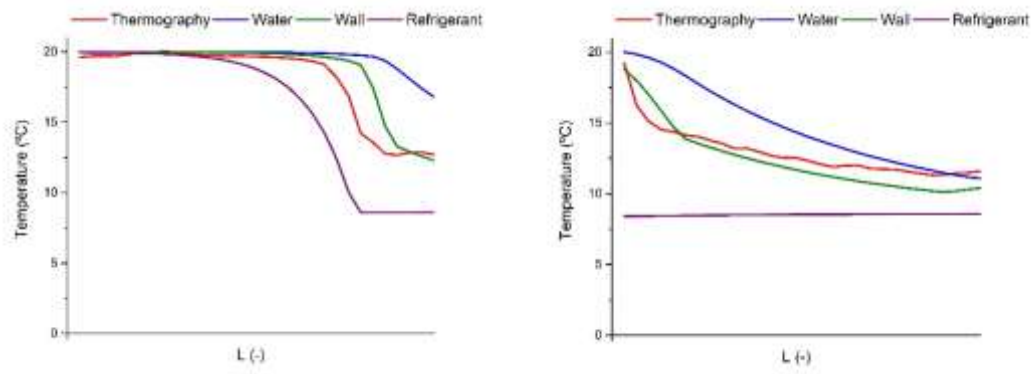

Figure 8. Comparison between the calculated temperature evolution and the one corresponding to the thermography for the test point with x_{in}=0.14, SH=5 K and dTw=5 K, for part I (left), and part II (right).

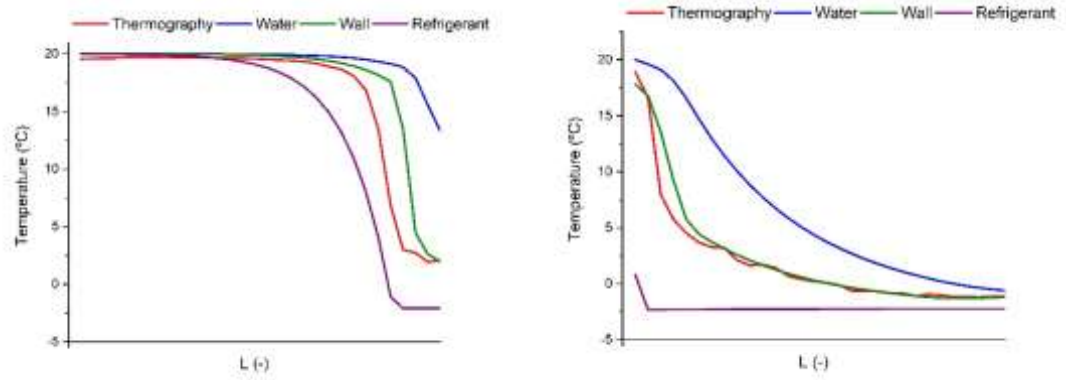

Figure 9. Comparison between the calculated temperature evolution and the one corresponding to the thermography for the test point with x_{in}=0.20, SH=15 K and dTw=13 K, for part I (left), and part II (right).

As it can be observed in Figures 7, 8 and 9, the readings from the thermographies seem to agree quite well with the temperature evolution of the plates, and the thermography temperature always approaches the water outlet temperature at the bottom of the evaporator, what makes perfectly sense if one takes into account that the thermographies are taken from the side where the edges of the plates are brazed. The comparison clearly shows the large difference of the temperature evolution of water and refrigerant between part I of the evaporator and part II. While in part I, most of the evaporator area is used for superheating the vapor, in part II, the whole area must be employed to evaporate the refrigerant liquid.

If one now compares Figure 8 and Figure 9, it becomes evident the reason why, with a similar maldistribution of refrigerant, in the case of *dTw*=5 K the penalty of the maldistribution (T_{evap} = 8.4ºC) is much lower than in the case of *dTw*=13 K (T_{evap} = -2.31 ºC), the reason is the huge

temperature drop of the water across part II water channels in the case of *dTw*=13 K. This huge temperature drop, of 21.5 K, is caused because the largest fraction of the liquid refrigerant is sent to part II channels, where, at the same time only 1/3 of the water channels (in this case) are available to provide the heat required for its evaporation, resulting in a huge decrease of the water temperature, and correspondingly of the evaporation temperature.

So, in summary, the maldistribution causes that most of the liquid refrigerant concentrates in only one part of the channels of the evaporator, what, not only decreases proportionally the heat transfer area available for the evaporation, but additionally, decreases proportionally the available water flowrate for providing the necessary heat for that evaporation. Both effects, combined together, are the ones conditioning the evaporation temperature.

Therefore, the penalty of the maldistribution on the evaporation performance strongly depends on the availability of the secondary fluid in the channels, or region, where most of the refrigerant liquid is concentrated. In the studied case, given a certain refrigerant maldistribution, its penalty on the evaporator performance could be diminished if, in some way, the water flow rate through the channels of part II could be increased, either by increasing the total flow rate (lower *dTw*), or by having a non-even distribution of the water flow rate among the channels which sends a higher flow towards the channels of Part II of the evaporator. For instance, in this second case, by entering the water to the evaporator from the opposite side to the refrigerant, or by redesigning the water distributor header.

It is important to mention that, this combined effect of reduction of available area and reduction of the secondary fluid availability, is also happening in other evaporator designs. A good example of those are the minichannel evaporators which typically suffer from refrigerant maldistribution. The problem of the maldistribution of the refrigerant being amplified by the reduction of the airflow which they are able to capture around those channels full of liquid refrigerant, leading to a local high drop of the air temperature around them, and therefore to a low evaporation temperature, which also would cause a much sooner start and much more active frosting process around those channels.

Finally, it should be mentioned that the described data reduction methodology, based on the analysis of the thermography and the measured evaporator performance is suitable to give an estimate of the maldistribution which seem reasonable and consistent with the observed data. The methodology could be standardized in the following way. When maldistribution is suspected, a short series of tests (maybe only 3 should be enough in order to see the variability of the estimation, and averaging the results) around the system operation point (given superheat and inlet quality) with decreasing water flow rate, keeping constant, as is has been done in the present study, the water inlet temperature. Values above 10 K temperature drop across the evaporator are recommended, for instance 12, 14 K. As it can be observed in Table 1, at those values the outlet of the water temperature of part II are just 1 K above the evaporation temperature. With that information, the measured evaporation temperature, the other measured parameters, the estimation from the thermography of the fraction of channels which seem being flooded with liquid, and the value of the minimum temperature in the thermography, it is possible, by solving the indicated system of equations to estimate the maldistribution index.

4. Conclusions

The thermographies have shown that about 1/3 of the refrigerant channels in the studied evaporator, the ones at the other side of the refrigerant inlet port, seem to be fed with a high fraction of the liquid refrigerant. Those channels clearly show much lower temperatures in the thermographies indicating that the evaporation of the refrigerant takes almost all the height of the channels up to the top, even at high superheats. This is a result more or less valid for all tested conditions with the exception of the tests with null superheat which seem to have a fairly even refrigerant distribution.

The degradation of the evaporator performance is clearly higher when the water temperature drop across the evaporator is higher. Very low values of the evaporation temperature, which would lead to a significant *COP* drop, are obtained at the case with the highest tested water temperature drop (dTw = 13K). This degradation of the evaporator performance is not so high at the highest tested inlet quality (x_{in} = 0.3), what is probably due to the good effect of the distributor orifices.

The highest degradation occurs at superheats around 8 K and vapor qualities between 0.12 and 0.22.

Maximum *COP* degradation is 10% for the case of water temperature drop 5 K, while it is 17% for the case of 13 K.

A special data reduction methodology has been devised to estimate the maldistribution of the refrigerant (maldistribution index ψ) by assuming that the evaporator can be divided in two parts; part I represents the group of channels where the inlet vapor quality is relative high and most of the heat transfer area is employed in superheating the vapor, while part II represents the group of channels where most of the liquid refrigerant concentrates (very low inlet vapor quality), and, in consequence, most of the heat transfer area is employed in the evaporation of the liquid refrigerant with very low or null superheating of the generated vapor

The estimated maldistribution index reaches a maximum about 1.6, meaning that the refrigerant mass flowrate through part II of the evaporator is 60% higher than the one it would circulate if there were even distribution of the refrigerant among the channels. The maldistribution index is considerable high at superheats higher than 4 K and refrigerant inlet qualities below 0.2, with little influence of the water temperature drop *dTw*. This estimation is qualitatively in good agreement with the analysis of the thermographies.

A comparison between the thermographies and the evolution of the water, refrigerant and plate temperatures, evaluated by means of a detailed evaporator model, for parts I and II of the evaporator, shows a good qualitative agreement; the readings from the thermographies seem to agree quite well with the temperature evolution of the plates, and the thermography temperature always approaches the water outlet temperature at the bottom of the evaporator, what makes perfectly sense if one takes into account that the thermographies are taken from the side where the edges of the plates are brazed. The comparison clearly shows the large difference of the temperature evolution of water and refrigerant from part I of the evaporator to part II. While in

part I, most of the evaporator area is used for superheating the vapor, in part II, the whole area must be employed to evaporate the refrigerant liquid.

An additional important conclusion is that the same maldistribution of refrigerant can lead to very different intensity of degradation of the evaporator performance, mainly depending on the water temperature drop across the evaporator. The reason for this being that, at the same time that the refrigerant liquid concentrates in a fraction of the refrigerant channels, the water flowrate available for the evaporation of the refrigerant in those channels, mostly liquid refrigerant, is diminished proportionally to the decrease of the number of channels, dealing to a huge 9temperature drop of the water flowing across those channels, which forces a big drop of the evaporation temperature.

Therefore, when there is a significant maldistribution of refrigerant in an evaporator, the effect of reduction of available area for the evaporation combines with the reduction of the secondary fluid flow rate, dramatically increasing the penalty of the maldistribution on the evaporator performance. This combined effect is not characteristic of BPHEs only, but of all evaporators, and it must be seriously considered in evaporators which have to work with high temperature drop in the secondary fluid side, as it is the case of waste heat recovery applications. Working with null superheat eliminates the problem, at the same time that allows reaching the maximum evaporation temperatures.

Acknowledgements

The authors would like to acknowledge the Spanish "MINISTERIO DE ECONOMIA Y COMPETITIVIDAD", through the project ref-ENE2014-53311-C2-1-P-AR "Aprovechamiento del calor residual a baja temperatura mediante bombas de calor para la produccion de agua caliente" for the given support.

References

Bach, C.K., Groll, E.A., Braun, J.E., Horton, W.T., 2013. Application of a hybrid control of expansion valves to a domestic heat pump and a walk-in cooler refrigeration system. HVAC&R Res. 19, 800–813. https://doi.org/10.1080/10789669.2013.822251

Brix, W., Kærn, M.R., Elmegaard, B., 2010. Modelling distribution of evaporating CO2 in parallel minichannels. Int. J. Refrig. 33, 1086–1094.

https://doi.org/https://doi.org/10.1016/j.ijrefrig.2010.04.012

Brix, W., Kærn, M.R., Elmegaard, B., 2009. Modelling refrigerant distribution in microchannel evaporators. Int. J. Refrig. 32, 1736–1743. https://doi.org/10.1016/J.IJREFRIG.2009.05.006

Chisholm, D., 1983. Two-phase flow in pipelines and heat exchangers. London : Godwin.

Choi, J.M., Payne, W.V., Domanski, P.A., 2003. Effects of Non-Uniform Refrigerant and Air Flow Distributions on Finned- Tube Evaporator Performance. Int. Congr. Refrig. ICR0040.

Corberán, J.M., De Córdoba, P.F., Gonzálvez, J., Alias, F., 2001. Semiexplicit method for wall temperature linked equations (sewtle): A general finite-volume technique for the calculation of complex heat exchangers. Numer. Heat Transf. Part B Fundam. 40, 37–59. https://doi.org/10.1080/104077901300233596

Corberan, J.M., Gonzalvez, J., Montes, P., Blasco, R., Corberán, J.M., Gonzálvez, J., Montes, P., Blasco, R., 2002. 'ART' A Computer Code To Assist The Design Of Refrigeration and A/C Equipment. Int. Refrig. Air Cond. Conf. 1–8.

García-Cascales, J.R., Vera-García, F., Corberán-Salvador, J.M., Gonzálvez-Maciá, J., 2007. Assessment of boiling and condensation heat transfer correlations in the modelling of plate heat exchangers. Int. J. Refrig. 30, 1029–1041. https://doi.org/https://doi.org/10.1016/j.ijrefrig.2007.01.004

Gong, J., Gao, T., Yuan, X., Huang, D., 2008. Effects of air flow maldistribution on refrigeration system dynamics of air source heat pump chiller under frosting conditions. Energy Convers. Manag. 49, 1645–1651. https://doi.org/https://doi.org/10.1016/j.enconman.2007.11.004

Jin, S., Hrnjak, P., 2017. A new method to simultaneously measure local heat transfer and visualize flow boiling in plate heat exchanger. Int. J. Heat Mass Transf. 113, 635–646. https://doi.org/https://doi.org/10.1016/j.ijheatmasstransfer.2017.04.116

Kærn, M.R., Brix, W., Elmegaard, B., Larsen, L.F.S., 2011. Performance of residential air-conditioning systems with flow maldistribution in fin-and-tube evaporators. Int. J. Refrig. 34, 696–706. https://doi.org/10.1016/J.IJREFRIG.2010.12.010

Li, W., Hrnjak, P., 2018. An experimentally validated model of single-phase flow distribution in brazed plate heat exchanger. 17th Int. Refrig. Air Cond. Conf. Purdue.

Mader, G., Palm, B., Elmegaard, B., 2015. Maldistribution in air–water heat pump evaporators. Part 1: Effects on evaporator, heat pump and system level. Int. J. Refrig. 50, 207–216. https://doi.org/https://doi.org/10.1016/j.ijrefrig.2014.07.006

Mancini, R., Zühlsdorf, B., Aute, V., Markussen, W.B., Elmegaard, B., 2019. Performance of heat pumps using pure and mixed refrigerants with maldistribution effects in plate heat exchanger evaporators. Int. J. Refrig. 104, 390–403. https://doi.org/10.1016/J.IJREFRIG.2019.05.023

Navarro-Peris E, Alvarez-Piñeiro L, Albaladejo P, Schnabel L, Corberan JM. Refrigerant maldistribution in BPHE evaporators. Part A: Testing campaign and experimental results. Submitted for publication to International Journal of Refrigeration

Stevanovic, V., Cucuz, S., Carl-Meissner, W., Maslovaric, B., Prica, S., 2012. A numerical investigation of the refrigerant maldistribution from a header towards parallel channels in an evaporator of automotive air conditioning system. Int. J. Heat Mass Transf. 55, 3335–3343. https://doi.org/https://doi.org/10.1016/j.ijheatmasstransfer.2012.02.071

Vist, S., Pettersen, J., 2004. Two-phase flow distribution in compact heat exchanger manifolds. Exp. Therm. Fluid Sci. 28, 209–215. https://doi.org/10.1016/S0894-1777(03)00041-4